Anonymous Referee #2

This study performed ground measurements in a small city at the very south end of continental China along the South China Sea. The authors attempted to attribute the sources from the composition and absorption measurements using receptor models, however the analysis of the entire study is rough and the conclusions are vague for the current version.

Response: The authors appreciate the reviewer's valuable suggestions, and we believe that the revised manuscript has been significantly improved after considering the comments. Below are point-to-point responses.

- Many pieces of essential work are missing, which should all appear in the main figures. I only list a few examples: the time series as classified by clusters, the diurnal variations of absorption for each cluster (to exclude the possible local sources), complete statistics of all parameters are required (BC mass, AAE, PM, compositions). Please do a complete and sound analysis and just show it. Otherwise, the conclusions are based on nowhere.

Response: We thank the reviewer for pointing out the shortcoming of our manuscript. Following the reviewer's suggestion, we have added a Fig. R1 below (also see Fig. 1 in the revised main text) to show the time series of light absorption (Abs(λ)) influenced by different clusters, a Fig. R2 below (also see Fig. S10 in the revised supporting information) to show the diurnal variations of Abs(λ) of each cluster, a Table R1 below (also see Table 1 in the revised manuscript) to summarize the optical parameters, and a Table R2 below (also see Table 2 in the revised main text) to summarize the mass concentrations of $PM_{2.5}$ and chemical species.

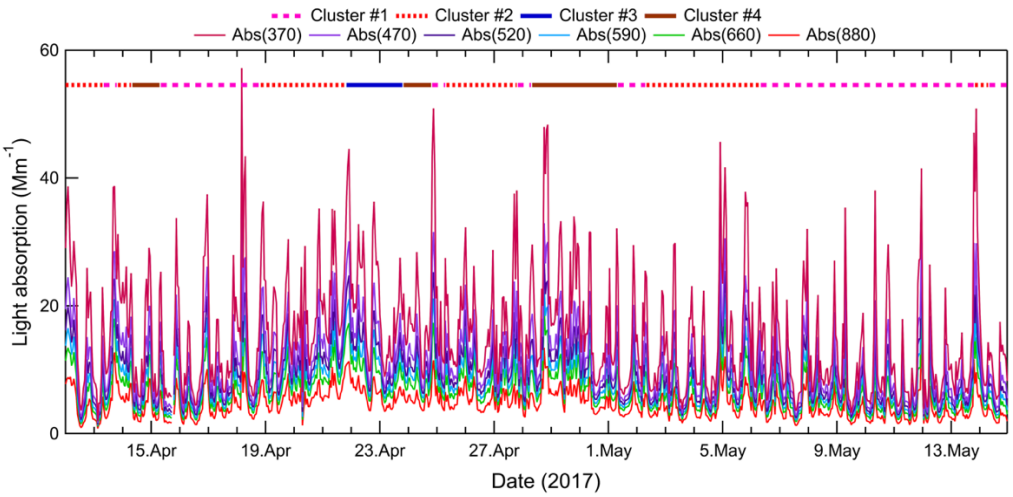

Figure R1. Time series of hourly averaged light absorption at different wavelengths (Abs(λ), λ = 370, 470, 520, 590, 660, and 880 nm). The different types of horizontal lines represent the four clusters of air masses.

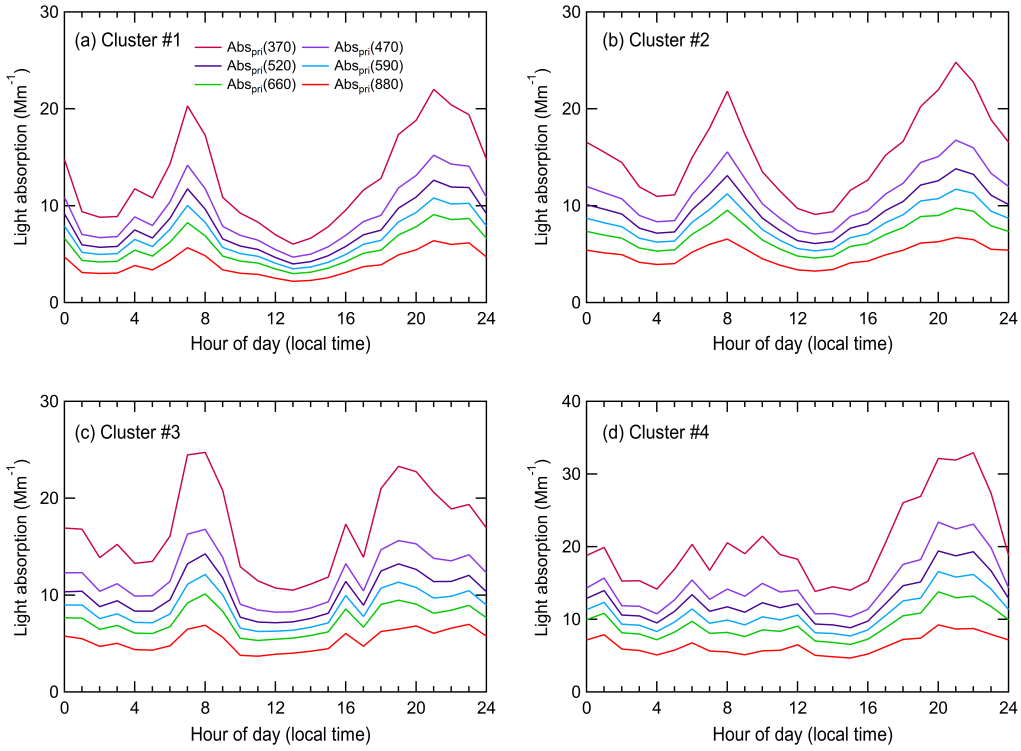

Figure R2. Diurnal variations of light absorption from primary emissions ($Abs_{pri}(\lambda)$, λ = 370, 470, 520, 590, 660, and 880 nm) in different clusters.

Table R1. Summary of light absorption at different wavelengths (Abs(λ), λ = 370, 470, 520, 590, 660, and 880 nm) and absorption Ångström exponent (AAE) of different emission sources.

Parametera	Average	Standard deviation
Abs(370) (Mm^{-1})	15.7	5.3
Abs(470) (Mm^{-1})	11.4	3.7
Abs(520) (Mm^{-1})	9.7	3.0
Abs(590) (Mm^{-1})	8.3	2.6
Abs(660) (Mm^{-1})	7.0	2.2
Abs(880) (Mm^{-1})	4.9	1.5
AAEtotal	1.41	0.05
AAEship	1.06	0.03
AAEbiomass	1.75	0.06
AAEvehicle	0.96	0.06

[a]AAE_{total} represents the AAE caused by total light-absorbing aerosols while AAE_{ship}, $AAE_{biomass}$, and $AAE_{vehicle}$ are AAE from ship emissions, biomass burning, and motor vehicle emissions, respectively.

Table R2. The average mass concentrations of carbonaceous matter, water-soluble ions, inorganic elements, and organics during the campaign.

Types	Species	Average	Standard deviation
$PM_{2.5}$ ($\mu g\ m^{-3}$)		14.3	4.2
Carbonaceous matter ($\mu g\ m^{-3}$)	organic carbon	2.7	1.1
	elemental carbon	0.8	0.3
Water-soluble ions ($\mu g\ m^{-3}$)	Na^+	0.5	0.2
	NH_4^+	0.6	0.4
	K^+	0.2	0.1
	Mg^{2+}	0.05	0.02
	Ca^{2+}	0.2	0.1
	Cl^-	0.23	0.2
	NO_3^-	0.6	0.3
	SO_4^{2-}	3.5	1.2
Inorganic elements ($ng\ m^{-3}$)	Ti	13.1	9.7
	V	2.4	1.4
	Mn	5.1	2.7
	Fe	127.3	78.9
	Ni	1.1	0.6
	Cu	28.0	14.4
	Zn	16.6	11.1
	Br	2.6	2.0
Organics ($ng\ m^{-3}$)	hopanes	0.2	0.05

- many issues here regarding the source attribution. The local source influence needs to be clearly excluded, or by some way to show it is of minor influence compared to the regional sources you stated.

Response: We thank the reviewer pointing out the influence of local emissions. Our sampling site is not located at a background area, therefore the influence of local emissions cannot be neglected. As a coastal city near the South China Sea, one of our objectives is to emphasize the ship emissions transported from ocean. Given that the air masses from the South China Sea are unable to carry pollutants from biomass burning, motor vehicles, and fugitive dust, these sources were possibly mainly

influenced by local emissions. In the revised manuscript, we used diurnal patter and concentration-weighted trajectory (CWT) analysis to indicate the influences of local emissions and regional transport. We have reworked the relevant discussion to make it more clearly, and it now reads as follows:

"To identify the possible source areas that affected $Abs_{pri}(\lambda)$, CWT analysis was performed based on the three-day backward trajectories. Large CWT values were mainly concentrated in the South China Sea (Fig. S9), highlighting the effect of ship emissions on aerosol light absorption. Additionally, the three-day backward trajectories were grouped into four cluster-mean trajectories to investigate the impact of different sources on $Abs_{pri}(\lambda)$ (Fig. 4). The air masses associated with Cluster #1 originated from the South China Sea. The $Abs_{ship}(\lambda)$ was the largest contributor in this cluster constituting 44–45% of $Abs_{pri}(\lambda)$ due to the high vessel traffic density over the South China Sea, consistent with the CWT results. Cluster #1 accounted for about 44% of the total trajectories, suggesting that Sanya was subjected to the influence of ship exhaust-related LAC aerosols, transported from the South China Sea. It is noteworthy that the diurnal pattern of $Abs_{pri}(\lambda)$ showed typically high values in the mornings and evenings (Fig. S10). This was attributed to the daily anthropogenic activities and variations in height of the planetary boundary layer. Given that the air masses from the South China Sea are unable to carry pollutants from biomass burning, motor vehicles, and fugitive dust, these sources were possibly mainly influenced by local emissions.

Cluster #2 originated from the South China Sea near the Indochina Peninsula and accounted for 35% of the total trajectories. The $Abs_{ship}(\lambda)$ was also vital in this cluster, accounting for 34–37% of $Abs_{pri}(\lambda)$. Fig. S10 shows that the $Abs_{pri}(\lambda)$ of Cluster #2 displayed a similar diurnal trend as that of Cluster #1. Considering that the air masses of Cluster #2 also originated from the South China Sea, the sources except for ship emissions were mainly influenced by local discharge. A small number of air masses were grouped into Cluster #3 and Cluster #4, accounting for only 6% and 15% of total trajectories, respectively. Cluster #3

originated from southern Burma and passed over Thailand, Laos, and Vietnam. On the other hand, Cluster #4 had the longest cluster-mean trajectory which originated and passed through the coastal areas of South-eastern China. Biomass burning was the dominant contributor to $Abs_{pri}(\lambda)$ in both clusters, with 62–69% for Cluster #3 and 56–64% for Cluster #4. Moreover, the $Abs_{biomass}(\lambda)$ of Cluster #3 and Cluster #4 were 1.8–4.4 times higher than those of Cluster #1 and Cluster #2. Since the $Abs_{biomass}(\lambda)$ from Cluster #1 and Cluster #2 were mainly attributed to local emissions, the higher values in Cluster #3 and Cluster #4 may have been influenced by the long-range transport of biomass burning from Southeast Asia and South-eastern China, where there was a large number of fire incidences (Fig. 4)."

Not clear with the definition of secondary substance, most organic and mineral should also be primary?

Response: The organics contains primary emissions and secondary formation, and the mineral dust here is fugitive dust. In our study, we used the BC-tracer method with MRS approach to distinguish the light absorption contributed by primary emissions (including black carbon and primary brown carbon) and secondary formation (that is secondary brown carbon). As the results shown in the main text, ~95% of light absorption was contributed by primary emissions. The reason why we wanted to prove this was that there was lack of tracers of secondary brown carbon when we did the PMF model. The negligible impact of secondary formation on light absorption can avoid potential uncertainty of not obtaining the secondary brown carbon in the optical source apportionment. However, the minor light absorption of secondary BrC did not mean that the mass concentration of secondary organic aerosol was low. It only indicated that few secondary organic aerosols had the light-absorbing ability. To eliminate the misunderstanding on this aspect, we revised our original expressions to "Based on Eq. (5), $Abs_{sec}(\lambda)$ accounted for less than 5% of $Abs(\lambda)$ (Table S1), suggesting a negligible impact of secondary formation on the light absorption capacity of aerosols during the study. Therefore, the uncertainty caused by using only $Abs_{pri}(\lambda)$ in the model could be

put to rest in the absence of an effective way to identify the source of secondary BrC."

Where did the dust come from, I don't think there was any dust sources rather than some sea salt.

Response: We agree with the reviewer that the sea salt is an important component in particulate matter at coastal city. However, the sea salt is a scattering material which is beyond the scope of our study. Here the dust denotes the fugitive dust which was mainly caused by the winds or relevant human activities in Sanya. In order to make it more clearly, we have changed the 'mineral dust' to 'fugitive dust' in the revised manuscript.

The shipping emissions are not really supported with any other external data source (I don't know what is that because I can't see anything from the current analysis done so far).

Response: We agree with the reviewer that more external tracers of ship emissions can further strengthen the identification results. However, the tracers were hard to determine due to the lack of effective chemical analysis method in this study. Actually, the V is a reliable tracer to indicate the ship emissions used in previous studies (e.g., Tao et al., 2016; Mamoudou et al., 2018). The V/Ni ratio can be further used to identify the ship emissions because it varies from 2.5 to 4.0 for this source (Cesari et al., 2014). In the case of lack of other external tracers, the current used V-based identification method in PMF model is also a reliable approach. To strengthen the reliability of our results, we have added more description about the verification of the PMF in the revised manuscript (see next response below).

References:

Cesari, D., Genga, A., Ielpo, P., Siciliano, M., Mascolo, G., Grasso, F. M., and Contini, D.: Source apportionment of $PM_{2.5}$ in the harbour–industrial area of Brindisi (Italy): Identification and estimation of the contribution of in-port ship emissions, Sci. Total Environ., 497–498, 392–400, https://doi.org/10.1016/j.scitotenv.2014.08.007, 2014.

Mamoudou, I., Zhang, F., Chen, Q., Wang, P. and Chen, Y.: Characteristics of PM2.5

from ship emissions and their impacts on the ambient air: A case study in Yangshan Harbor, Shanghai, Sci. Total Environ., 640–641, 207–216, https://doi.org/10.1016/j.scitotenv.2018.05.261, 2018.

Tao, J., Zhang, L., Cao, J., Zhong, L., Chen, D., Yang, Y., Chen, D., Chen, L., Zhang, Z., Wu, Y., Xia, Y., Ye, S. and Zhang, R.: Source apportionment of PM2.5 at urban and suburban areas of the Pearl River Delta region, south China - With emphasis on ship emissions, Sci. Total Environ., 574, 1559–1570, https://doi.org/10.1016/j.scitotenv.2016.08.175, 2017.

- The PMF analysis seems not quite convincing, could you provide more details about the scenarios.

Response: Following the reviewer's suggestion, we have added more descriptions about the verification of the PMF results (e.g., BS, DISP, and BS-DISP analysis) in the revised manuscript. It now reads as follows:

"Moreover, two to seven factors were selected to initiate the PMF5.0 run. Due to the additional factors, the Q/Q_{exp} ratio decreased with the increased number of factors as shown in Fig. S7. The decrease in Q/Q_{exp} was large when the factor number changed from 2 to 3 and 3 to 4 but stabilized as the factor number grew larger than 4, indicating that four factors may be the optimal solution. After multiple runs of the PMF5.0 model, four factor sources including ship emissions, motor vehicle emissions, biomass burning, and fugitive dust were finally identified (Fig. 3a). Additionally, the modeled $Abs_{pri}(\lambda)$ at different wavelengths showed strong correlations with the measured $Abs(\lambda)$ ($r = 0.82–0.89$, $p < 0.01$, Fig. S8). The slopes of 0.92–0.98 were consistent with the absorption fractions of $Abs_{pri}(\lambda)$ estimated by the BC-tracer method combined with the MRS approach (Table S1). The scaled residuals for each species varied between -3 and +3.

The uncertainty of each factor profile was further evaluated using BS, DISP, and BS-DISP. The BS results showed that the reproducibility of each source factor

was larger than 80% (Table S2), indicating good stability. Therefore, this suggested that the four source factors were appropriate. No swaps occurred in DISP, indicating the stability of the selected solution. Furthermore, all BS-DISP runs were successful. Overall, these results pointed to the efficiency of the PMF5.0 model in performing optical source apportionment."

And even so, would you really believe to incorporate the spectral absorption in parallel with the offline composition will really give some physical meaning? There seems no signature of sources on the absorption.

Response: We agree with the reviewer that there is no special signature of sources for one single-wavelength light absorption. However, when we use multiwavelength light absorption data together (e.g., λ = 370, 470, 520, 590, 660, and 880 nm in this study), there will be certain indication for specific sources due to the different light-absorbing aerosols having distinct absorption properties. For example, brown carbon, which is mainly from biomass burning, absorbs light towards short wavelengths (e.g., near-ultraviolet region). Therefore, compared to the fossil fuel sources, the biomass burning can contribute more to light absorption in the near-ultraviolet region (e.g., λ = 370 nm). Moreover, this contribution decreases with increase in wavelength. In contrast, the motor vehicle emissions contribute less to light absorption at λ = 370 nm than biomass burning due to the presence of large amounts of black carbon. This contribution increases with increase in wavelength. From this perspective, the additional multiwavelength absorption data in the PMF model will be helpful for optimizing the performance of source apportionment.

The time resolution is different between online and offline measurements, did you just average the online data into a very low time interval.

Response: Yes, we averaged the period of online data to match each filter sampling time. In the revised manuscript, we have added a sentence to clarify this:

"Online $Abs_{pri}(\lambda)$ data was integrated to match each filter sampling time."

- MAC of organic should be normalized by organic matter (including all elements) not only organic carbon. The MAC of organic here doesn't mean anything.

Response: We followed the reviewer's suggestion and changed to discuss the MAC of organic matter instead of organic carbon. The relevant content in the main text and figure (Fig. 6 in the revised manuscript) were revised accordingly. The update calculation method in the revised manuscript is shown as follows:

"Additionally, MAC could be used to reflect the light absorption capacity of aerosols. The MACs of BC and BrC at different wavelengths ($MAC_{BC}(\lambda)$ and $MAC_{BrC}(\lambda)$, respectively) were calculated with $Abs_{BC}(\lambda)$ and $Abs_{BrC}(\lambda)$ divided by the corresponding mass concentrations of BC and organic matter (OM), respectively:

$$MAC_{BC}(\lambda) = \frac{Abs_{BC}(\lambda)}{[BC]} \quad (7)$$

$$MAC_{BrC}(\lambda) = \frac{Abs_{BrC}(\lambda)}{[OM]} \quad (8)$$

where the mass concentration of OM was estimated by a factor of 1.8 times that of OC mass concentration (Turpin and Lim, 2001)."

- I am not convinced with the forcing calculation and the directly correlated heating. I don't think you really need to make that calculation as the main job of this study is to get the absorption attribution properly. The forcing largely replies on the vertical distribution of AOD and SSA, which you don't really have such information, which is beyond the scope of this study though.

Response: We thank the reviewer pointing out this. The direct radiative effect (DRE) caused by light-absorbing carbonaceous (LAC) aerosols is mainly related to their light absorption properties. So, it will be valuable for further estimating the source-specific LAC DRE after we obtained the light absorption of different sources. We agree with the reviewer that aerosol DRE strongly relies on the vertical distributions of AOD and SSA. The Optical Properties of Aerosols and Clouds (OPAC) model is a mature and widespread approach used in current studies to retrieve the vertical AOD and SSA based

on the surface measurements of chemical composition (e.g., Singh et al., 2018; Zhao et al., 2019; Kant et al., 2020). In our study, we used the OPAC model combining the measured mass concentrations of OC, EC, and water-soluble ions as well as the estimated mineral dust to estimate the vertical AOD, SSA, and AP. These optical parameters are essential inputs in the SBDART model for calculation of aerosol DRE. After careful consideration, we think that the reviewer's puzzle may be caused by our original unclear description in models of OPAC and SBDART. Therefore, we added more information about the calculations of OPAC (e.g., compared with the PAX measured light extinction and the satellite-derived AODs) and SBDART model in the revised manuscript. It now reads as follows:

"**2.7 The Optical Properties of Aerosols and Clouds (OPAC) Model**

The OPAC model was used to retrieve the following parameters: aerosol optical depth (AOD), single scattering albedo (SSA), and asymmetric parameter (AP). The parameters were important in estimating the radiative effect of aerosols. A detailed description of the OPAC software package was given by Hess et al. (1998). The measured mass concentrations of OC, EC, and water-soluble ions as well as the estimated mineral dust loading (=[Fe]/0.035) during the day were used in the OPAC model to estimate the optical parameters. Moreover, the BC number concentration in the OPAC model was constrained by the measured BC mass concentration. Although several water-soluble ions and mineral dust were obtained, they did not contain all the water-soluble and insoluble material. Therefore, based on the measured data, the number concentrations of water-soluble and insoluble materials were tuned. This was done until the differences between the OPAC-derived light scattering, light absorption, and SSA versus the corresponding PAX-measured values were within 5% (Fig. S3). After the aerosol light extinction coefficient (sum of light scattering and absorption) was obtained, the AOD was estimated as follows (Hess et al., 1998):

$$\mathrm{AOD} = \sum_j \int_{H_{j,min}}^{H_{j,max}} \sigma_{e,j}(h)dh = \sum_j \sigma_{e,j}^1 N_j(0) \int_{H_{j,min}}^{H_{j,max}} e^{-\frac{h}{Z_j}} dh \quad (12)$$

where $H_{j,max}$ and $H_{j,min}$ were the upper and lower boundaries in layer j; $\sigma_{e,j}$

was the surface aerosol light extinction coefficient in layer j; h was the layer height; $\sigma_{e,j}^{1}$ represented the aerosol light extinction coefficient that was normalized to 1 particle cm^{-3}; N_j was the number concentration in layer j; and Z was the scale height. Furthermore, the OPAC-derived AODs were tuned to match the satellite-derived AODs (https://giovanni.gsfc.nasa.gov/giovanni, last access: January 2020) by altering the scale height in OPAC until the difference between them was within 5%. Owing to closure with AOD and anchoring of chemical composition, the assumptions in the OPAC model did not have a significant impact on the estimation of radiative effect in subsequent section 2.8 (Satheesh and Srinivasan 2006).

2.8 Estimations of radiative effect and heating rate

The LAC direct radiative effect (DRE) was estimated by the Santa Barbara DISORT (Discrete Ordinate Radiative Transfer) Atmospheric Radiative Transfer (SBDART) model in the shortwave spectral region of 0.25–4.0 μm. A detailed description of the SBDART model was given by Ricchiazzi et al. (1998). The AOD, SSA, and AP are essential input parameters in the SBDART model and were obtained from the OPAC model (see section 2.7). In addition to these, several other input parameters were included, namely the surface albedo, solar zenith angle, and profiles of atmospheric parameters. The surface albedo was derived from the Moderate Resolution Imaging Spectroradiometer (https://modis-atmos.gsfc.nasa.gov/ALBEDO/index.html, last access: January 2020). On the other hand, the solar zenith angle was calculated with a specific time and location (i.e., latitude and longitude) using a small code from the SBDART model. Furthermore, six standard atmospheric vertical profiles (i.e., tropical, mid-latitude summer, subarctic summer, mid-latitude winter, subarctic winter and US62) were embedded in the SBDART model. They provided vertical distributions of temperature, pressure, water vapor, and ozone density (Ricchiazzi et al., 1998). In this study, the mid-latitude summer was selected to represent the situation of Sanya based on its classification as a mid-latitude

region. Obregón et al. (2015) demonstrated that the SBDART model could provide a reliable estimation of radiative effect. Moreover, aerosol DRE was defined as the difference in the radiation flux (F) either at the Earth's surface or at the top of the atmosphere, respectively with and without the aerosol in the atmosphere:

$$DRE = (F\downarrow - F\uparrow)_{\text{with aerosol}} - (F\downarrow - F\uparrow)_{\text{without aerosol}} \quad (13)$$

where $\downarrow$ and $\uparrow$ represented the downward and upward flux, respectively. Atmospheric DRE was then estimated by the difference between the DRE at the top of the atmosphere and the Earth's surface.

Further, the atmospheric heating rate ($\frac{\partial T}{\partial t}$, in unit of K d^{-1}) caused by LAC aerosols was estimated using the first law of thermodynamics and hydrostatic equilibrium as follows (Liou, 2002):

$$\frac{\partial T}{\partial t} = \frac{g}{C_p} \times \frac{\Delta F}{\Delta P} \quad (14)$$

where $\frac{g}{C_p}$ was the lapse rate and g stood for acceleration due to gravity while C_p described the specific heat capacity of air at a constant pressure (1006 J kg^{-1} K^{-1}). Additionally, ΔF was the atmospheric DRE contributed by LAC aerosols and ΔP represented the atmospheric pressure difference (300 hPa)."

References:

Kant, Y., Shaik, D. S., Mitra, D., Chandola, H. C., Babu, S. S. and Chauhan, P.: Black carbon aerosol quantification over north-west Himalayas: Seasonal heterogeneity, source apportionment and radiative forcing, Environ. Pollut., 257, 113446, https://doi.org/10.1016/j.envpol.2019.113446, 2020.

Singh, S., Tiwari, S., Hopke, P. K., Zhou, C., Turner, J. R., Panicker, A. S. and Singh, P. K.: Ambient black carbon particulate matter in the coal region of Dhanbad, India, Sci. Total Environ., 615, 955–963, https://doi.org/10.1016/j.scitotenv.2017.09.307, 2018.

Zhao, S., Yu, Y., Yin, D., Yu, Z., Dong, L., Mao, Z., He, J., Yang, J., Li, P. and Qin, D.: Concentrations, optical and radiative properties of carbonaceous aerosols over

urban Lanzhou, a typical valley city: Results from in-situ observations and numerical model, Atmos. Environ., 213, 470–484, https://doi.org/10.1016/j.atmosenv.2019.06.046, 2019.

- No need such redundant description for the trajectory clustering, as this is not your original work and has been so widely used previously, which was just output using some user-friendly software.

Response: Following the reviewer's suggestion, we briefly described the method of trajectory cluster analysis in the revised manuscript. It now reads as follows:

"Cluster analysis of three-day backward air-mass trajectories was used to investigate the impact of transport pathways on Abs(λ). The backward trajectories were calculated hourly with an arrival height of 500 m above ground level using the Hybrid Single-Particle Lagrangian Integrated Trajectory Model (Draxler and Rolph, 2003). The cluster analysis was performed according to the angle-based distance statistics method (Q. Wang et al., 2018a). Furthermore, a Concentration-weighted Trajectory (CWT) analysis based on the three-day backward trajectories was used to identify the potential source areas (Q. Wang et al., 2016). Finally, cluster and CWT analyses were performed using a GIS-based TrajStat software developed by Wang et al. (2009)."